Research Article

Benzyl Alcohol Valorization via the In Situ Production of Reactive Oxygen Species

Gregory Sharp,[△] Richard J. Lewis,*[,△] Junhong Liu, Guiseppina Magri, David J. Morgan, Thomas E. Davies, Ángeles López-Martín, Rong-Jian Li, Callum R. Morris, Damien M. Murphy, Andrea Folli, A. Iulian Dugulan, Liwei Chen, Xi Liu,* and Graham J. Hutchings*

Read Online

ACCESS | Metrics & More | Article Recommendations | SI Supporting Information

ABSTRACT: In this contribution, we outline the efficacy of Pd-based bimetallic catalysts toward the oxidative upgrading of benzyl alcohol via the in situ synthesis of H_2O_2 (and related reaction intermediates) from the elements. In particular, the formation of PdAu and PdFe nanoalloys is observed to be highly effective, offering high yields of benzaldehyde and near total selectivity to the desired product, with these catalysts outperforming alternative materials reported in the literature. Notably, the PdFe formulation also achieves high selective utilization of H_2, a key requirement if the in situ approach to chemical synthesis is to become economically viable. Correlative studies, focusing on the direct synthesis of H_2O_2 and further experiments utilizing preformed H_2O_2, coupled with Electron Paramagnetic Resonance (EPR) spectroscopy indicate that H_2O_2 itself is not primarily responsible for the observed catalysis, but rather, the performance of the PdAu and PdFe formulations can be related to the generation of reactive oxygen species (ROS). While the origin of these ROS is not fully understood, it is hypothesized that they are generated through a combination of (i) the desorption of reaction intermediates formed during H_2O_2 synthesis and (ii) through Fenton-mediated chemistry involving the synthesized H_2O_2, in the case of the PdFe-based materials. Importantly, our EPR studies also identify the noninnocent nature of the reaction solvent.
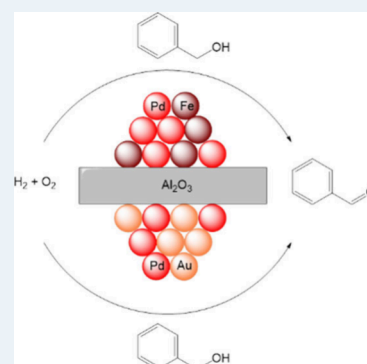
KEYWORDS: Alcohol Oxidation, Hydrogen Peroxide, Palladium−Gold, Palladium−Iron, Reactive Oxygen Species, Noninnocent Solvent

INTRODUCTION

The one-pot synthesis and utilization of H_2O_2 for the selective valorization of platform chemicals represents an attractive alternative to the use of conventional stoichiometric oxidants (e.g., permanganate and dichromate), commercial H_2O_2 and high-temperature aerobic routes. Indeed, if implemented at scale, such chemistry could achieve significant financial and environmental improvements as a result of process intensification and the decoupling of oxidative transformations from the means by which conventional oxidants, including H_2O_2, are produced on an industrial scale.[1,2]

The selective oxidation of primary alcohols, such as benzyl alcohol (Scheme 1), to the corresponding aldehyde, is of particular industrial importance, with the products of such transformations widely utilized in the pharmaceutical and perfumery industries, or as agrochemicals.[3] Typically, the industrial oxidation of benzyl alcohol relies on the utilization of stoichiometric oxidants, with concerns around poor atom efficiency and the formation of large quantities of byproducts prompting interest in the application of benign oxidants, such as oxygen, through which high yields of benzaldehyde can be achieved. However, for aerobic upgrading to be effective relatively high reaction temperatures are often required, diminishing the environmental credentials which may be

associated with the use of oxygen as the terminal oxidant.[4−6] Alternatively, the application of commercial H_2O_2 has been demonstrated to allow for significantly lower reaction temperatures than that required when using oxygen, while also obtaining high selectivity toward desired products, with the synthesis of highly reactive oxygen species (ROS) such as $O_2^{•−}$, $•OH$, and $•OOH$ from H_2O_2, considered to be responsible for the initial proton abstraction from the alcohol moiety, which is necessary for aldehyde formation.[7,8] Clearly, numerous environmental and financial benefits may be realized if an alternative approach could be developed in which H_2O_2 and oxygen-based radical species including hydroxyl ($•OH$) and hydroperoxyl ($•OOH$) are generated in situ via the activation of O_2 through reaction with H_2.
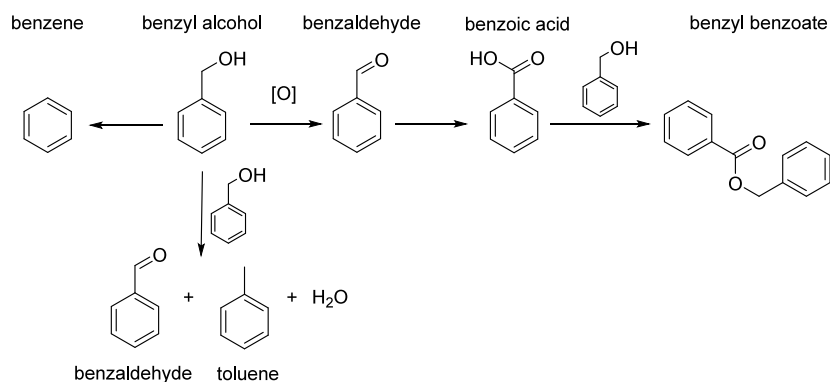
Supported PdAu nanoalloys have received significant attention for the in situ oxidation of numerous feedstocks,[9,10]

Scheme 1. General Reaction Pathway for the Oxidation of Benzyl Alcohol

with this, in part, stemming from the high reactivity of such materials toward the direct synthesis of H_2O_2,[11−13] with recent studies highlighting the crucial role of Au in promoting the desorption of H_2O_2,[14] as well as reaction intermediates[15] from catalytic surfaces. Additional works, including by our laboratory, have demonstrated the efficacy of coupling in situ H_2O_2 synthesis with Fenton(-like) pathways, where secondary metal species including Fe, Cu, Co, and Mn activate synthesized H_2O_2 to produce short-lived, but highly reactive oxygen species, which are comparable to those generated as reaction intermediates during the direct synthesis of H_2O_2.[16−18] However, to date, the interest in applying such in situ/Fenton systems to oxidative valorization has been limited, with those studies which have been disclosed typically reporting relatively low activities.[19]

For an in situ approach to chemical synthesis to rival alternative routes (i.e., those utilizing stoichiometric agents, molecular O_2, or preformed H_2O_2) significant improvements in catalyst performance are clearly required. Indeed, with the notable exception of recent reports into in situ ketone ammoximation,[2,20] a major drawback associated with the in situ approach to feedstock valorization is associated with the unselective utilization of H_2, through a combination of H_2O_2 hydrogenation to H_2O, and the formation of hydrogenated byproducts. The purification of resulting complex product streams, in addition to poor H_2 utilization, represents considerable hurdles to the commercialization of the in situ approach to oxidative valorization and overcoming these drawbacks has been a major focus of the community.

With the potential for ROS to be generated directly from the combination of H_2 and O_2 (i.e., as reaction intermediates during H_2O_2 synthesis) or through the Fenton-mediated decomposition of H_2O_2, we were motivated to explore the efficacy of these two approaches to ROS synthesis for the selective oxidation of a major platform chemical, benzyl alcohol to the corresponding aldehyde.

■ MATERIALS AND METHODS

Catalyst Preparation. Mono- and bi-metallic 1% Pd-X/Al_2O_3 catalysts (where Pd: X = 1:1 and X= Au, Mn, Fe, Co, Cu, Ru, Zn, Pt) have been prepared (on a weight basis) by an excess-chloride coimpregnation procedure, based on a methodology previously reported in the literature.[21] This method has been shown to result in an enhanced dispersion of metals, in particular Au, when compared to conventional impregnation procedures.[22] The procedure to produce 0.5%Pd-0.5%Au/Al_2O_3 (2 g) is outlined below, with a similar methodology

being utilized for all mono- and bi-metallic catalysts, using chloride-based metal precursors in all cases. The requisite amount of metal precursors used for the synthesis of the mono- and bi-metallic catalysts is reported in Table S1.

An aqueous acidified $PdCl_2$ solution (1.667 mL, 6 mg mL^{-1}, 0.58 M HCl, Merck) and aqueous $HAuCl_4 \cdot 3H_2O$ solution (0.8263 mL, 12.25 mg mL^{-1}, Strem Chemicals) were mixed in a 50 mL round-bottom flask and heated to 65 °C with stirring (1000 rpm) in a thermostatically controlled oil bath, with total volume fixed to 16 mL using H_2O (HPLC grade, Fischer Scientific). Upon reaching 65 °C, γ-Al_2O_3 (1.98 g, Fischer Scientific) was added over the course of 5 min with constant stirring. The resulting slurry was stirred at 65 °C for a further 15 min, after which the temperature was raised to 95 °C for 16 h to allow for complete evaporation of water. The resulting solid was mechanically ground prior to heat treatment in a reductive atmosphere (flowing 5%H_2/Ar, 500 °C, 4 h, and ramp rate of 10 °C min^{-1}).

X-ray diffractograms of key as-prepared catalysts are reported in Figure S1, with no reflections associated with active metals, indicative of the relatively low total loading and high dispersion of the immobilized metals. Surface area measurements, as determined by 5-point N_2 adsorption, are reported in Table S2.

Catalyst Testing. Note 1: The reaction conditions used within this study operate below the flammability limits of gaseous mixtures of H_2 and O_2.[23]

Note 2: The conditions used within this work for H_2O_2 synthesis and degradation have previously been investigated, where the presence of CO_2 as a diluent for reactant gases and methanol as a cosolvent has been identified as key to maintaining high catalytic efficacy toward H_2O_2 production.[24] In particular, the CO_2 gaseous diluent, has been found to act as an in situ promoter of H_2O_2 stability through dissolution in the reaction solution and the formation of carbonic acid. We have previously reported that the use of the CO_2 diluent has a comparable promotive effect to that observed when acidifying the reaction solution to a pH of 4 using HNO_3.[25]

Note 3: In all cases reactions were run multiple times, over multiple batches of catalyst, with the data presented as an average of these experiments. Catalytic activity toward H_2O_2 synthesis and H_2O_2 degradation was found to be consistent to within ±2% based on multiple reactions. For the in situ oxidation of benzyl alcohol, product yield was observed to be consistent to within ±4% based on multiple reactions.

Direct Synthesis of H_2O_2. Hydrogen peroxide synthesis activity was evaluated using a Parr Instruments stainless steel

autoclave with a nominal volume of 50 mL and a maximum working pressure of 2000 psi. To test each catalyst for H_2O_2 synthesis, the autoclave was charged with catalyst (0.01 g), solvent (5.6 g methanol, HPLC grade, Fisher Scientific) and H_2O (2.9 g, HPLC grade, Fisher Scientific). The charged autoclave was then purged three times with 5% H_2/CO_2 (100 psi) before filling with 5%H_2/CO_2 to a pressure of 420 psi, followed by the addition of 25%O_2/CO_2 (160 psi). The reaction mixture was stirred (1200 rpm) for 0.5 h, with the temperature being maintained at 20 °C. Reactor temperature control was achieved using a HAAKE K50 bath/circulator using an appropriate coolant. The reactor was not continuously supplied with reagent gases. H_2O_2 productivity was determined by titrating aliquots of the final solution after reaction with acidified $Ce(SO_4)_2$ (0.01 M) in the presence of ferroin indicator. Catalyst productivities are reported as $mol_{H_2O_2} \, kg_{cat}^{-1} \, h^{-1}$.

Degradation of H_2O_2. Catalytic activity toward H_2O_2 degradation (via hydrogenation and decomposition pathways) was determined in a manner similar to that used for measuring the H_2O_2 direct synthesis activity of a catalyst. The autoclave was charged with methanol (5.6 g, HPLC grade, Fisher Scientific), H_2O_2 (50 wt %, 0.69 g, Merck), H_2O (2.21 g, HPLC grade, Fisher Scientific) and catalyst (0.01 g), with the solvent composition equivalent to a 4 wt % H_2O_2 solution. From the solution, two aliquots of 0.05 g were removed and titrated with acidified $Ce(SO_4)_2$ solution using ferroin as an indicator to determine an accurate concentration of H_2O_2 at the start of the reaction. The charged autoclave was then purged three times with 5%H_2/CO_2 (100 psi) before filling with 5%H_2/CO_2 (420 psi). The reactor was not continuously supplied with reagent gases. The reaction mixture was stirred (1200 rpm) for 0.5 h, with the reaction temperature maintained at 20 °C. After the reaction was complete, the catalyst was removed from the reaction solvents via filtration and as described previously, two aliquots of 0.05 g were titrated against the acidified $Ce(SO_4)_2$ solution using ferroin as an indicator. Catalyst degradation activity is reported as $mol_{H_2O_2} \, kg_{cat}^{-1} \, h^{-1}$.

Benzyl Alcohol Oxidation via In Situ Production of H_2O_2. The oxidation of benzyl alcohol has been investigated in a 50 mL Parr Instruments stainless steel autoclave. The autoclave was charged with catalyst (0.01 g), methanol (7.13 g, HPLC grade, Fisher Scientific,) and benzyl alcohol (1.04 g, 9.62 mmol, Merck) along with 0.5 mL of the internal standard mesitylene (0.43 g, 3.58 mmol, Merck). The charged autoclave was then purged three times with 5% H_2/CO_2 (100 psi) before filling with 5% H_2/CO_2 to a pressure of 420 psi, followed by the addition of 25%O_2/CO_2 (160 psi). The pressures of 5% H_2/CO_2 and 25%O_2/CO_2 were taken as gauge pressures. The reactor was subsequently heated to 50 °C, followed by stirring at 1200 rpm for 0.5 h, unless otherwise stated. The reactor was not continuously supplied with reagent gases. After the reaction was complete the reactor was cooled in ice water to a temperature of 15 °C, after which a gas sample was analyzed by gas chromatography using a Varian CP-3380 equipped with a TCD detector and a Porapak Q column, to allow for determination of H_2 conversion. Subsequently, the catalyst was removed from the reaction solvents via filtration and liquid product yield was determined by gas chromatography using a Varian 3200 GC, equipped with a CP Wax 42 column and FID. The concentration of residual H_2O_2 was determined by

titrating aliquots of the final solution after reaction with acidified $Ce(SO_4)_2$ (0.01 M) in the presence of ferroin indicator.

The total capacity of the autoclave was determined via water displacement to allow for accurate determination of H_2 conversion and H_2 selectivity. When equipped with the PTFE liner and liquid reagents the total available gaseous space within the autoclave and is equivalent to 2.8 mmol of H_2.

H_2 conversion (eq 1), benzyl alcohol conversion (eq 2), product yield (eq 3), and H_2 selectivity toward benzaldehyde (eq 4) are defined as follows:

$$H_2 \text{ conversion } (\%) = \frac{mmol_{H_2(t(0))} - mmol_{H2(t(1))}}{mmol_{H_2(t(0))}} \times 100 \tag{1}$$

$$\begin{aligned} &\text{Benzyl alcohol conversion } (\%) \\ &= \frac{\text{Benzyl alcohol reacted (mmol)}}{\text{Benzyl alcohol initial (mmol)}} \times 100 \end{aligned} \tag{2}$$

$$\text{Product yield } (\%) = \frac{\text{Product (mmol)}}{\text{Benzyl alcohol initial (mmol)}} \times 100 \tag{3}$$

$$H_2 \text{ selectivity} = \frac{\text{Benzaldehyde (mmol)}}{H_2 \text{ conversion (mmol)}} \times 100 \tag{4}$$

Comparative experiments were conducted using commercial H_2O_2 (50 wt %, Merck), at a concentration equal to that produced if all H_2 in a standard reaction was selectively converted to H_2O_2.

To probe the contribution of alternative pathways to benzyl alcohol conversion (i.e., via aerobic or reductive pathways), an identical procedure to that outlined above for the oxidation of benzyl alcohol was followed, with the reactor charged with 5% H_2/CO_2 (420 psi) or 25% O_2/CO_2 (160 psi) reagent gases, total pressure was maintained at 580 psi using CO_2.

Gas Replacement Experiments for the Oxidation of Benzyl Alcohol via the In Situ Production of H_2O_2. An identical procedure to that outlined above for the in situ oxidation of benzyl alcohol was followed for a reaction time of 0.5 h. After this, stirring was stopped and the reactant gas mixture was vented prior to replacement with the standard pressures of 5%H_2/CO_2 (420 psi) and 25% O_2/CO_2 (160 psi). The reaction mixture was then stirred (1200 rpm) for a further 0.5 h. To collect a series of data points, it should be noted that individual experiments were carried out and the reactant mixture was not sampled online.

Hot Filtration Experiments for the Oxidation of Benzyl Alcohol via the In Situ Production of H_2O_2. An identical procedure to that outlined above for the oxidation of benzyl alcohol was followed for a reaction time of 0.5 h, with the exception that the reactor was not cooled to 15 °C, prior to the venting of gaseous reagents, rather the stirring was stopped and the gaseous reagents immediately removed. The solid catalyst was likewise removed from the "hot" post-reaction solution via filtration. The solution temperature after filtration was observed to decrease to 40 ± 2 °C. The post-reaction solution was then returned to the reactor to identify the contribution of leached species to the observed activity. Further experiments were conducted, where a fresh 1%Pd/ TiO_2 catalyst was added to the reaction mixture prior to running the reaction for a further 0.5 h.

Table 1. Catalytic Activity of PdAu Catalysts Towards the Direct Synthesis and the Subsequent Degradation of H_2O_2, as a Function of Catalyst Support[a]

Catalyst	Productivity $(mol_{H_2O_2}\ kg_{cat}^{-1}\ h^{-1})$	H_2O_2Conc. (wt %)	H_2Conv. (%)	H_2O_2Sel. (%)	Rate of reaction $(mmol_{H_2O_2}\ mmol_{metal}^{-1}\ h^{-1})$	Degradation $(mol_{H_2O_2}\ kg_{cat}^{-1}\ h^{-1})$
0.5%Pd-0.5%Au/TiO₂	80	0.16	42	35	1.11×10^3	503
0.5%Pd-0.5%Au/Al₂O₃	61	0.12	54	19	8.37×10^2	416
0.5%Pd-0.5%Au/CeO₂	20	0.04	18	2	2.79×10^2	284
0.5%Pd-0.5%Au/Nb₂O₅	19	0.03	4	86	2.65×10^2	40
0.5%Pd-0.5%Au/ZrO₂	9	0.02	11	13	1.22×10^2	268
0.5%Pd-0.5%Au/C (G60)	13	0.03	58	4	1.82×10^2	425

[a]H_2O_2 direct synthesis reaction conditions: catalyst (0.01 g), H_2O (2.9 g), MeOH (5.6 g), 5%H_2/CO_2 (420 psi), 25%O_2/CO_2 (160 psi), 0.5 h, 20 °C, 1200 rpm. H_2O_2 degradation reaction conditions: catalyst (0.01 g), H_2O_2 (50 wt.% 0.68 g), H_2O (2.22 g), MeOH (5.6 g), 5%H_2/CO_2 (420 psi), 0.5 h, 20 °C, 1200 rpm.

Radical Trapping Experiments with Electron Paramagnetic Resonance Spectroscopy. The catalyst (0.01 g) and solvent (methanol (7.1 g, HPLC grade, Fisher Scientific) or water (7.13 g, HPLC grade, Fisher Scientific)) were added to the reactor along with 5,5-dimethyl-1-pyrroline N-oxide (12 μL, Merck). The reactor was purged three times with 5%H_2/CO_2 (100 psi) and then filled with 5% H_2/CO_2 (420 psi) and 25%O_2/CO_2 (160 psi). The reactor was then heated to 50 °C and once the temperature was reached, stirring (1200 rpm) was commenced for 0.5 h. Once the reaction was complete, the reactor was purged with 20 bar N_2 for 20 min before the catalyst was separated by filtration and the filtered solution loaded into a 1.1 mm quartz tube for analysis by EPR spectroscopy.

Various blank reactions were also analyzed by EPR spectroscopy to determine any background activity or signals.

Continuous wave (CW) X-band EPR spectra were recorded at 298 K using a Bruker EMX Micro spectrometer equipped with a Bruker ER 4123d dielectric resonator. Spectra were recorded at ca. 9.75 GHz and 2 mW microwave power, with 100 kHz field modulation frequency, 1 G field modulation amplitude, 5×10^4 receiver gain, 10.00 ms conversion time and 5.02 ms time constant. EPR spectra were simulated using the EasySpin toolbox running within the MathWorks Matlab environment.[26]

Catalyst Characterization. A Kratos Axis Ultra-DLD photoelectron spectrometer was used to collect X-ray photoelectron spectra utilizing monochromatic Al Kα X-ray source operating at 144 W (12 mA × 12 kV). Data was collected using the Hybrid analysis mode over a rectangular analysis area of approximately 700 × 300 μm and at pass energies of 40 and 160 eV for high-resolution and survey spectra, respectively. Sample charging effects were minimized through low energy electrons and all data subsequently calibrated to the C(1s) of adventitious carbon taken to be 284.8 eV, which gave a Al(2p) value of 74.6 ± 0.1 eV, typical for Al_2O_3. All data was processed using CasaXPS v2.3.20 rev 1.2H using a Shirley background and modified Wagner sensitivity factors as supplied by the instrument manufacturer. Fitting was achieved using models taken from bulk compounds (Pd and Au metal foils and PdO). The Au(4f) peaks fit on top of Ti loss structure and also Pd(4s) signal, to account for this background broad, constrained Voight function was used to model these underlying peaks.

Brunauer−Emmett−Teller (BET) surface area measurements were conducted using a Quadrasorb surface area analyzer. A 5-point isotherm of each material was measured using N_2 as the adsorbate gas. Samples were degassed at 250 °C for 2 h prior to the surface area being determined by 5-point N_2 adsorption at −196 °C, and data analyzed using the BET method.

The bulk structure of the catalysts was determined by powder X-ray diffraction using a ($\theta-\theta$) PANalytical X'pert Pro powder diffractometer using a Cu Kα radiation source, operating at 40 keV and 40 mA. Standard analysis was carried out using a 40 min run with a backfilled sample, between 2θ values of 10−80°. Phase identification was carried out using the International Centre for Diffraction Data (ICDD).

Total metal leaching from the supported catalyst was quantified via inductively coupled plasma mass spectrometry (ICP-MS). Postreaction solutions were analyzed using an Agilent 7900 ICP-MS equipped with I-AS autosampler. All samples were diluted by a factor of 10 using HPLC grade H_2O (1% HNO_3 and 0.5% HCl matrix). All calibrants were matrix-matched and measured against a five-point calibration using certified reference materials purchased from PerkinElmer and certified internal standards acquired from Agilent.

DRIFTS measurements were taken on a Bruker Tensor 27 spectrometer fitted with a mercury cadmium telluride (MCT) detector. A sample was loaded into the Praying Mantis high temperature (HVC-DRP-4) in situ cell before exposure to N_2 and then 1% CO/N_2 at a flow rate of 50 cm³ min⁻¹. A background spectrum was obtained using KBr, and measurements were recorded every 1 min at room temperature. Once the CO adsorption bands in the DRIFT spectra ceased to increase in size, the gas feed was changed back to N_2 and measurements were repeated until no change in subsequent spectra was observed.

Aberration-corrected scanning transmission electron microscopy (AC-STEM) was performed using a probe-corrected S/TEM instrument (Hitachi HF5000), operating at 200 kV. The instrument was equipped with an annular dark field (ADF) detector, a secondary electron detector and dual Oxford Instruments XEDS detectors (2 × 100 mm²) having a total collection angle of 2.02 sr.

Transmission ⁵⁷Fe Mössbauer spectra were collected at 300 and 4.2 K with a conventional constant-acceleration spectrometer using a ⁵⁷Co(Rh) source. Velocity calibration
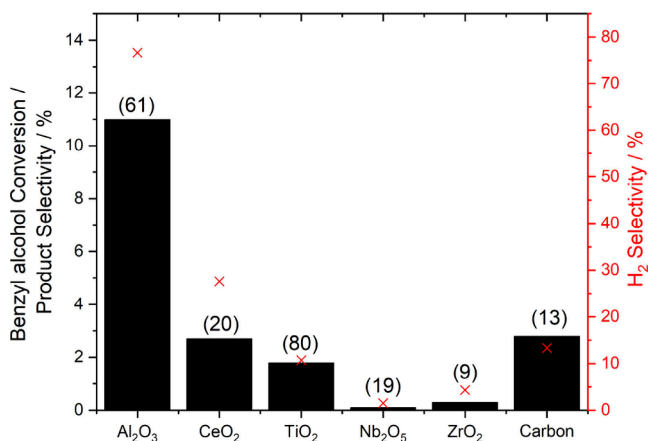
was carried out using an α-Fe foil at room temperature. The Mössbauer spectra were fitted using the Mosswinn 4.0 program.[27]

RESULTS AND DISCUSSION

Our initial studies established the efficacy of a series of PdAu nanoalloy catalysts, prepared on a range of supports, via an excess-chloride coimpregnation procedure,[21] toward the direct synthesis and subsequent degradation of H_2O_2 (Table 1). Importantly, previous studies have demonstrated that the support is not wholly benign in the direct synthesis reaction, offering activity toward competitive H_2O_2 degradation pathways[28] as well as controlling nanoalloy morphology, particle size, and the speciation of active metals, particularly Pd.[29] Indeed, there exists an extensive body of literature that has investigated the role of the support in achieving high selectivity in the direct synthesis of H_2O_2.

As reported previously a strong dependency between catalytic performance and the nature of the support was observed,[29] with the enhanced activity of the 0.5%Pd-0.5%Au/ TiO_2(P25) catalyst toward H_2O_2 formation (80 $mol_{H_2O_2}$ kg_{cat}^{-1} h^{-1}), in comparison to alternative formulations, clearly observed. Indeed the rate of H_2O_2 synthesis observed over the 0.5%Pd-0.5%Au/TiO_2 catalyst is particularly noteworthy given the ambient reaction temperatures utilized and the relative instability of H_2O_2 even under such mild conditions, with the application of subambient temperatures typically utilized to inhibit competitive degradation reactions and improve H_2O_2 selectivity.[30]

Interestingly it was not possible to draw a direct correlation between catalytic activity toward H_2O_2 direct synthesis and the in situ oxidation of benzyl alcohol (Figure 1, with additional data reported in Table S3). Indeed, while it may have been
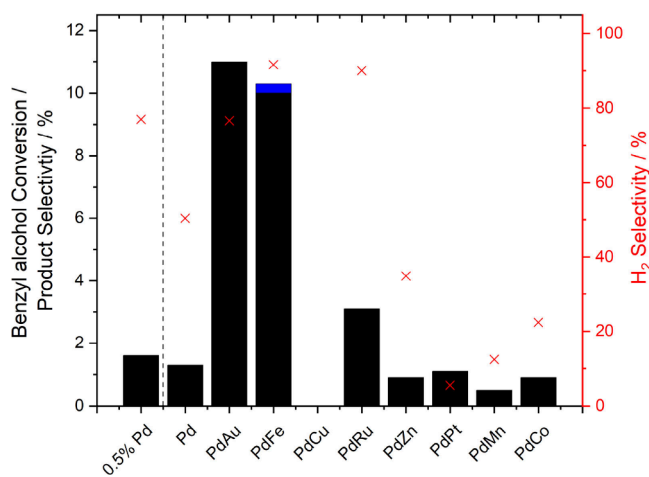
expected that the 0.5%Pd-0.5%Au/TiO_2 catalyst would offer superior activity toward benzyl alcohol valorisation, compared to alternative formulations, based on H_2O_2 synthesis rates alone, the CeO_2 (2.7% product yield), carbon (G60) (2.8% product yield) and notably γ-Al_2O_3 (11.0% product yield) supported catalysts were found to considerably outperform the TiO_2 analogue (1.8% product yield), despite the increased H_2O_2 synthesis activity of the latter formulation (Table 1). While it is important to note the difference in reaction conditions utilized for both studies, such observations indicate that, in the case of in situ benzyl alcohol oxidation, H_2O_2 may not be the primary species responsible for the observed catalysis. Notably, similar observations have been made for alternative oxidative transformations which proceed via in situ H_2O_2 synthesis and a proton abstraction mediated by oxygen-based radials.[31]

While PdAu-based formulations have been widely investigated for both the aerobic oxidation of a range of feedstocks[2,32−35] and the direct synthesis of H_2O_2[21,36] in recent years a growing focus has been placed on the replacement of Au, and the alloying of Pd with a range of more abundant transition metals.[29,37,38] Indeed this has been a particular focus for direct H_2O_2 production with a range of catalyst formulations identified that offer exceptional selectivities toward the oxidant, with improvements often associated with the disruption of contiguous Pd ensembles and the modification of Pd oxidation states.[39−43]

With these earlier works in mind, and using a γ-Al_2O_3 support, we next investigated the efficacy of a range of Pd-based bi-metallic formulations toward both the in situ oxidation of benzyl alcohol (Figure 2, with additional data reported in Table S4) and the direct synthesis of H_2O_2 (Table S5). These secondary metals were selected due to their known ability to promote Fenton-type pathways (i.e., the decom-

Figure 1. Effect of support on the activity of PdAu-based catalysts toward the selective oxidation of benzyl alcohol via the in situ H_2O_2 production and the direct synthesis of H_2O_2. Key: benzaldehyde (black bars); H_2 selectivity toward benzaldehyde (red crosses). In-situ oxidation of benzyl alcohol reaction conditions: catalyst (0.01 g), benzyl alcohol (1.04 g, 9.62 mmol), MeOH (7.1 g), 5%H_2/CO_2 (420 psi), 25%O_2/CO_2 (160 psi), 50 °C, 0.5 h, 1200 rpm. H_2O_2 direct synthesis reaction conditions: catalyst (0.01 g), H_2O (2.9 g), MeOH (5.6 g), 5%H_2/CO_2 (420 psi), 25%O_2/CO_2 (160 psi), 0.5 h, 20 °C, 1200 rpm. Note: Values in parentheses represent catalytic activity toward H_2O_2 direct synthesis (as $mol_{H_2O_2}$ kg_{cat}^{-1} h^{-1}). H_2 selectivity was determined, based on the mol of H_2 utilized in the formation of benzaldehyde.

Figure 2. Catalytic activity of bimetallic 0.5%Pd-0.5%X/Al_2O_3 catalysts toward the selective oxidation of benzyl alcohol via in situ H_2O_2 synthesis, as a function of secondary metal modifier. Key: benzaldehyde (black bars), benzoic acid (blue bars); H_2 selectivity toward benzaldehyde (red crosses). Reaction conditions: catalyst (0.01 g), benzyl alcohol (1.04 g, 9.62 mmol), MeOH (7.1 g), 5%H_2/CO_2 (420 psi), 25%O_2/CO_2 (160 psi), 50 °C, 0.5 h, 1200 rpm. Note: H_2 selectivity was determined, based on the mol of H_2 utilized in the formation of benzaldehyde. Comparisons were made to a 0.5%Pd/Al_2O_3 catalyst, where Pd loading was identical to that of the bimetallic analogues.

position of H_2O_2 to ROS), including Co, Mn, Cu, and Fe, and indeed, in many cases their application (with commercial H_2O_2) has been reported for the selective oxidation of primary alcohols.[7] Additionally, alternative metals which have been reported to enhance H_2O_2 synthesis rates, when alloyed with Pd (Au, Pt, Ru, Zn),[44] were exploited, with comparisons made to monometallic Pd catalysts, at metal loadings of 1 wt.% (i.e., identical to that of the bi-metallic analogues) and 0.5 wt.% (i.e., identical to the Pd loading present in the bi-metallic formulations).

Interestingly, the introduction of many of the secondary metals we have previously identified to improve the performance of Pd-based catalysts toward the in situ oxidation of benzyl alcohol[19] were found to have a limited promotive effect within this study, with the clear exception of Au. Notably, this earlier work also utilized the excess-chloride wet co-impregnation route to catalyst synthesis, which is used within this study, but focused on the application of TiO_2(P25) as catalyst support. Here we also highlight the comparable activity of the 0.5%Au-0.5%Pd/TiO_2 catalyst studied in this work (Figure 1) to that reported in our earlier investigation, under identical reaction conditions.[19] Such observations highlight the key role of the support in dictating catalyst performance, which is perhaps understandable given the numerous studies which have identified the control of nanoparticle composition and morphology, which can be obtained through careful selection of the nanoparticle carrier.[45] The introduction of Fe into the Pd-based catalyst was also found to result in a significant improvement in reactivity (10.3% benzyl alcohol conversion), compared to the monometallic Pd analogue (1.3% benzyl alcohol conversion). Indeed the 0.5%Pd-0.5%Fe/Al_2O_3 catalyst was found to offer benzyl alcohol conversion rates comparable to that observed over the 0.5%Pd-0.5%Au/Al_2O_3 formulation (11.0% benzyl alcohol conversion), with both catalysts significantly outperforming analogous formulations utilizing TiO_2(P25) as the carrier, under identical reaction conditions (2.8 and 5.6% benzyl alcohol conversion for PdAu/TiO_2 and PdFe/TiO_2 formulations, respectively).[19]

With the clear enhancement in catalytic activity identified upon the introduction of both Au and Fe into a supported Pd catalyst, we were motivated to investigate this subset of formulations (i.e., the 1%Pd/Al_2O_3, 0.5%Pd-0.5%Au/Al_2O_3, and 0.5%Pd-0.5%Fe/Al_2O_3 catalysts), in order to broaden our understanding of the underlying cause for the observed trends in catalytic performance.

It was subsequently determined that across the catalytic series, there were negligible contributions toward benzyl alcohol conversion when using a purely oxidative (25%O_2/CO_2) or reductive (5%H_2/CO_2) atmosphere (Figure S2). Such observations, particularly when utilizing an oxygen-only feed may be unsurprising given the low reaction temperatures employed in this study (50 °C), with temperatures exceeding 80 °C typically utilized for aerobic benzyl alcohol oxidation.[46−48] The formation of relatively low concentrations of benzaldehyde, in the presence of a H_2-only gaseous atmosphere, may be attributed to the incomplete purging of dissolved oxygen from the reaction medium prior to the reaction commencing. Notably, in the case of these latter experiments, we also observed the presence of toluene, the formation of which has been previously correlated with limited H_2O_2 formation rates.[49] Further investigations also revealed that a significant improvement in benzyl alcohol conversion may be obtained via an in situ approach compared to that

observed when using commercial H_2O_2 at a concentration comparable to that which would be obtained if all the H_2 in the system was selectively converted to H_2O_2. Such trends are likely associated with the complete addition of the preformed H_2O_2 at the start of the reaction, although the effect of proprietary stabilizing agents (often acids or halides), present in commercially available H_2O_2 should also be considered.[50] These observations further highlight the potential for oxygen-based radical species to be primarily responsible for the observed catalysis, rather than H_2O_2 itself.

A comparison of initial rates, at a reaction time (0.25 h), where there are assumed to be no limitations associated with gaseous reagent availability (i.e., H_2 conversion <30%), is presented in Table 2, with the comparable performance of the

Table 2. Comparison of Initial Rates of Benzyl Alcohol Oxidation via in-situ H_2O_2 Synthesis[a]

Catalyst	Reaction Rate (mmol$_{aldehyde}$ h^{-1})	Benzyl alcohol Conv. (%)	Benzaldehyde Sel. (%)	H_2 Conv. (%)	H_2 Sel. (%)
1%Pd/ Al_2O_3	0.3	0.9	100	6	52
1% PdAu/ Al_2O_3	2.2	5.8	100	27	75
1% PdFe/ Al_2O_3	2.2	6.1	100	23	92

[a]Reaction conditions: catalyst (0.01 g), benzyl alcohol (1.04 g, 9.62 mmol), MeOH (7.1 g), 5%H_2/CO_2 (420 psi), 25%O_2/CO_2 (160 psi), 50 °C, 0.25 h, 1200 rpm. Note: H_2 selectivity was determined based on the mol of H_2 utilized in the formation of benzaldehyde.

PdAu and PdFe formulations identified. Determination of H_2 selectivity (i.e., the mol of H_2 utilized in the in situ oxidation of benzyl alcohol to benzaldehyde), over the three formulations at this time point reveals the superior performance of the 0.5% Pd-0.5%Fe/Al_2O_3 catalyst (92% H_2 selectivity), compared to the 1%Pd/Al_2O_3 (52% H_2 selectivity) or 0.5%Pd-0.5%Au/Al_2O_3 (75% H_2 selectivity) analogues, clearly highlighting the beneficial role of Fe incorporation into Pd and to a lesser extent that of Au. Notably, such comparisons of catalyst selectivity over the PdAu and PdFe formulations are at near-identical rates of H_2 conversion, and so it is possible to conclude that trends in selectivity are not due to variation in this metric. The similarity in benzyl alcohol and H_2 conversion rates, but distinct variation in H_2 selectivity over the 0.5%Pd-0.5%Au/Al_2O_3 and 0.5%Pd-0.5%Fe/Al_2O_3 formulations are particularly interesting and may indicate differing intrinsic activity to individual steps within the overall reaction network (i.e., oxidant synthesis and utilization as well as successive degradation pathways). It is also important to note that the relative abundance of oxidative species (H_2O_2, $O_2^{\bullet-}$, $^{\bullet}OH$, and $^{\bullet}OOH$) generated over these formulations are likely to differ, with each contributing toward the overall catalysis to a lesser/greater extent. Notably, probing the catalytic activity toward H_2O_2 degradation (via decomposition and hydrogenation pathways), under conditions established for H_2O_2 stability (Table S5), does reveal distinct variation in catalytic selectivity toward H_2O_2, which in turn hints at the complex reaction network prevalent in this system.

In order to gain insight into the possible electronic modification of Pd species which may result from the formation of alloyed species, we subsequently analyzed the

catalytic series by X-ray photoelectron spectroscopy (Figure S3) and diffuse reflectance infrared Fourier transform spectroscopy, using CO as a probe molecule (Figure S4). Given the key role of the Pd oxidation state in determining catalytic performance toward H_2O_2 synthesis, such an understanding is key in rationalizing observed activity trends.[51] Interestingly, our XPS analysis reveals the presence of both Pd^0 and Pd^{2+} in the case of the Pd-only and PdAu formulations, whereas Pd^{2+} alone is observed for the PdFe bimetallic system (Figure S3). Such variation in Pd speciation may be surprising given the utilization of a reductive heat treatment during catalyst synthesis (5%H_2/Ar, 500 °C, 4 h, and ramp rate of 10 °C min^{-1}); however, these observations align well with our evaluation of similar catalyst formulations.[19] Furthermore, it should be noted that the Pd oxidation states of the as-prepared materials are likely not fully representative of those under reaction conditions. In the case of the PdFe catalyst we observe a distinct signal at a binding energy of 710.8 eV, characteristic of Fe^{3+} (Figure S5). However, here we wish to highlight the propensity of Fe to readily oxidize under ambient conditions and the inherent surface sensitivity of XPS. As such, we cannot rule out the presence of alternative Fe oxidation states based on our XPS analysis alone.

Subsequent investigation of this subset of catalytic materials by CO-DRIFTS (Figure S4), is perhaps unsurprisingly dominated by stretching modes associated with CO adsorbed onto Pd species. Focusing on the monometallic 1%Pd/Al_2O_3 catalyst two distinct bands are apparent, the first centered at higher wavenumbers (2000−2100 cm^{-1}), which can be assigned to CO bonded to low-coordination Pd sites (i.e., corner and edge sites), while the second, broader band centered at lower wavenumbers (1800−2000 cm^{-1}) represents the multifold adsorption of CO on contiguous Pd domains. Upon the introduction of either Au or Fe a definite blueshift to higher wavenumbers can be observed for both the low- and highly- coordinated CO species indicative of a strong electronic interaction between Pd and the secondary metal modifier, which aligns well with our XPS analysis. Notably, earlier studies into PdAu systems have reported a similar blueshift as a result of alloy formation and in particular the segregation of Pd within the alloy structure corresponding to the occupation of lower coordination sites.

With our evaluation by XPS unable to provide sufficient information about the nature of the Fe in the PdFe catalyst, we subsequently employed ^{57}Fe Mössbauer analysis to gain further insight. Notably, due to the relatively low loadings of active metals in our catalytic samples, we utilized model formulations of greater metal loading (2.5%Pd-2.5%Fe/Al_2O_3, with comparisons made to a monometallic 5%Fe/Al_2O_3 analogue) (Figure 3 and Table 3).

Interestingly, the spectra of the 5%Fe/Al_2O_3 sample was fitted with contributions from metallic Fe (magnetic sextuplet) and high-spin Fe^{2+} and Fe^{3+} species (paramagnetic doublets), with the Fe^{2+} hyperfine parameters indicative of the presence of a highly dispersed Fe species. By comparison, the 2.5%Pd-2.5%Fe/Al_2O_3 sample also contained Fe^{2+} and Fe^{3+} paramagnetic signals, but instead of the metallic Fe observed in the monometallic analogue, two magnetic sextuplets were measured, which may be assigned to Fe−Pd alloys of varying composition. In the case of both formulations, the paramagnetic Fe^{3+} signal consists of two components, indicating the presence of Fe oxide clusters and highly dispersed Fe^{3+} species that are still paramagnetic at analysis temperatures,
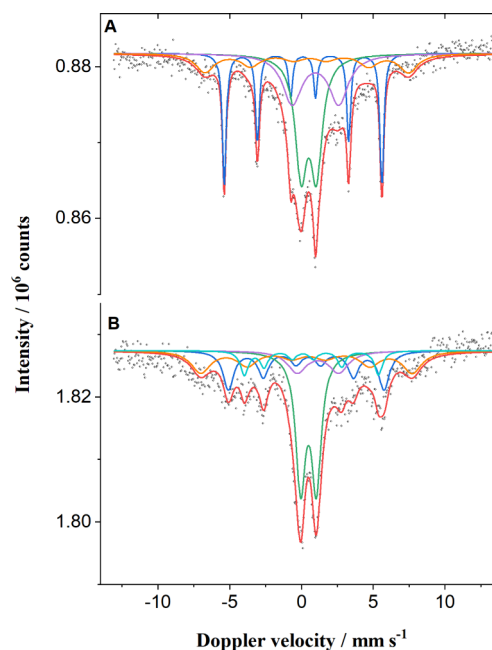
Figure 3. Mössbauer analysis of model 5%FePd/Al_2O_3 samples at 4.2 K: (A) 5%Fe/Al_2O_3 and (B) 2.5%Pd-2.5%Fe/Al_2O_3.

aligning well with our XPS analysis of the 0.5%Pd-0.5%Fe/Al_2O_3 formulation, where Fe^{2+} and Fe^{3+} species were observed.

Returning to our catalytic samples, we investigated the activity of key formulations over extended reaction times, as shown in Figure 4 (additional data are reported in Tables S6−8), with metal leaching over a standard reaction (0.5 h), as determined from ICP-MS analysis of post reaction solutions reported in Table S9. Notably, while the activity of the 0.5%Pd-0.5%Au/Al_2O_3 and 0.5%Pd-0.5%Fe/Al_2O_3 catalysts were comparable over the initial 45 min of reaction (approximately 12% benzyl alcohol conversion), and were indeed far greater than that observed over the 1%Pd/Al_2O_3 analogue (1.5% benzyl alcohol conversion), at extended reaction times a discernible variation in performance could be observed, with the increased performance of the PdFe catalyst clear (17.1% conversion at 1.5 h) when compared to the PdAu formulation (13.8% conversion at 1.5 h). Catalytic selectivity toward benzaldehyde appeared to be relatively consistent over all three formulations, with only small concentrations of benzoic acid (4% selectivity), detected over the 0.5%Pd-0.5%Fe/Al_2O_3 catalyst at relatively high conversion rates. Such observations align well with earlier studies which have identified the role of benzyl alcohol and other alcohols in suppressing the formation of further oxidation products.[52,53] Although it is important to highlight that in these previous works methanol, the solvent used in this study, was not found to inhibit the overoxidation of benzaldehyde. Notably, no toluene was observed over the catalyst series.

XPS analysis of catalysts used in the in situ benzyl alcohol oxidation reaction (1.5 h) (Figure S6), reveals an increase in the Pd^0 content over the course of the reaction, which is unsurprising given the reductive atmosphere used during the catalysis. In the case of the Pd-only and PdAu catalysts the shift in Pd^0:Pd^{2+} ratio upon use is similar, with this metric equilibrating at a value of approximately 2.3, whereas this ratio was somewhat lower for the FePd analogue (1.6). For this latter formulation, no observable change in Fe binding energy

Table 3. Mössbauer Fitted Parameters of the 5%PdFe/Al$_2$O$_3$ Samples, Obtained at 4.2 K[a]

Catalyst	IS (mm·s^{-1})	QS (mm·s^{-1})	Hyperfine field (T)	Γ (mm·s^{-1})	Phase	Spectral contribution (%)
Fe/Al$_2$O$_3$	0.11	–	34.1	0.32	Fe^0 (blue)	26
	0.98	3.24	–	1.61	Fe^{2+} (magenta)	24
	0.48	−0.20	44.1	1.54	Fe^{3+} (clusters) (orange)	17
	0.51	1.06	–	0.98	Fe^{3+} (dispersed) (green)	33
Pd−Fe/Al$_2$O$_3$	0.41	−0.15	33.7	0.89	Fe−Pd(I) (blue)	22
	0.40	0.59	29.0	0.65	Fe−Pd(II) (cyan)	10
	1.15	2.89	–	1.62	Fe^{2+} (magenta)	11
	0.43	−0.14	45.8	1.59	Fe^{3+} (clusters) (orange)	22
	0.49	1.09	–	0.82	Fe^{3+} (dispersed) (green)	35

[a]Experimental uncertainties: Isomer shift: I.S. ± 0.1 mm s^{-1}; Quadrupole splitting: Q.S. ± 0.1 mm s^{-1}; Line width: Γ ± 0.2 mm s^{-1}; Hyperfine field: ± 0.2 T; Spectral contribution: ± 5%. Note: Colors in parentheses refer to spectra reported in Figure 3.

(710.8 eV) was detected, indicating the presence of Fe^{3+} throughout the reaction, with the concentration and chemical state remaining consistent over the course of the reaction (Figure S5), although again we caveat this observation with the limitations of XPS analysis to fully discern Fe speciation.

Interestingly, both the 0.5%Pd-0.5%Au/Al$_2$O$_3$ and 0.5%Pd-0.5%Fe/Al$_2$O$_3$ catalysts displayed very similar H$_2$ conversion rates over the course of 1.5 h of reaction (Tables S6−8), with this metric reaching approximately 70% over both formulations. However, the improved efficacy of the 0.5%Pd-0.5%Fe/Al$_2$O$_3$ catalyst is clear with this formulation offering significantly improved selectivity based on H$_2$ (80% at 1.5 h) compared to the PdAu analogue (68% at 1.5 h), which aligns well with our earlier observations over shorter reaction times (Table 2). The high selectivity of the PdFe formulation is particularly noteworthy, given concerns associated with selective H$_2$ utilization for a range of alternative in situ oxidative transformations.[54]

Given the relatively high rates of H$_2$ conversion observed over extended reaction times, we next set out to determine the extent to which catalytic performance may be limited by gaseous reagent availability. Sequential in situ benzyl alcohol oxidation experiments were conducted, where the gaseous reagents were recharged at intervals of 0.5 h (Figure 5, with additional information reported in Table S10). A near linear increase in benzyl alcohol conversion rate was observed over all three formulations, which may suggest that the observed plateau in the performance of the PdAu catalyst at extended reaction times (Figure 4), was not a result of catalyst deactivation and rather may be attributed to the reaction becoming limited by H$_2$ availability. These studies also reveal the comparable reactivity of both 0.5%Pd-0.5%Au/Al$_2$O$_3$ and 0.5%Pd-0.5%Fe/Al$_2$O$_3$ catalysts, when not limited by the availability of gaseous reagents. However, the use of a batch testing regime and the potential for residual H$_2$O$_2$ to contribute to the observed catalysis does complicate such comparisons. Notably, the reactivity of our optimal catalysts significantly exceeds those previously reported in the literature (Table S11), highlighting the potential improvements in the in situ approach to benzyl alcohol valorization that may be achieved through rational catalyst design.

With a focus on the 0.5%Pd-0.5%Fe/Al$_2$O$_3$ catalyst, we subsequently conducted a series of hot-filtration studies in order to identify the potential contribution of homogeneous metal species to the observed catalytic activity (Figure S7). For these experiments, a standard 0.5 h reaction was conducted, after which the heterogeneous catalyst was removed via filtration and the filtrate returned to the reactor for a further

0.5 h, under standard reaction conditions (i.e., with the introduction of fresh reactant gases). No additional benzyl alcohol conversion was observed after the removal of the solid catalyst, which may indicate the lack of a homogeneous contribution to the observed reactivity. In order to determine if the inactivity observed in the hot-filtration experiment was a result of the limited activity of the homogeneous component to synthesize H$_2$O$_2$, an additional experiment was conducted, whereby after an initial 0.5 h reaction the heterogeneous catalyst was replaced with a Pd-only catalyst (1%Pd/Al$_2$O$_3$), ensuring that the total moles of Pd was identical to that in the bimetallic PdFe formulation. A minor improvement in total product yield was observed (11.5%), which is comparable to the sum of the PdFe/Al$_2$O$_3$ (10.3%) and Pd/Al$_2$O$_3$ (1.3%) catalysts when used independently in the in situ reaction, over 0.5 h. Based on these observations it is therefore possible to conclude that if there is a contribution of homogeneous metal species toward the observed catalysis such a contribution is negligible.

Investigation of the Pd-based catalysts via HAADF-STEM revealed a considerable variation in nanoparticle size and composition with catalyst formulation (Figures6−7). The Pd-only catalyst was found to consist of relatively large (10−20 nm) particles with no indication of the small clusters which may not have been expected based on previous investigations into similar formulations prepared by the excess-chloride impregnation procedure used within this study.[21,24] However, it should be noted that these earlier studies have almost exclusively focused on the use of a TiO$_2$(P25) carrier, with earlier observations demonstrating the key role of the support in dictating nanoparticle morphology and in turn catalytic performance. The 0.5%Pd-0.5%Fe/Al$_2$O$_3$ catalyst displayed a relatively wide particle size range, with much of the metal present as larger 10−20 nm nanoparticles or agglomerates in addition to nanoparticles of intermediate size (5−10 nm) and smaller (1−3 nm) clusters. XEDS mapping studies (Figure 7, with additional data reported in Figures S8−9), confirmed that both species exist as PdFe alloys, although there is a clear dependence between particle size and composition, with the smaller (1−3 nm) particles consisting of relatively equal concentrations of both metals, whereas the larger species are Pd-rich (Figure 7). Notably, such observations align well with our earlier Mössbauer analysis of model catalysts, which identified the presence of multiple PdFe environments (Figure 3, Table 3). By comparison, the introduction of Au was found to result in the formation of well-mixed nanoalloys of approximately 5−10 nm (Figure 7, with additional data reported in Figures S10−11).
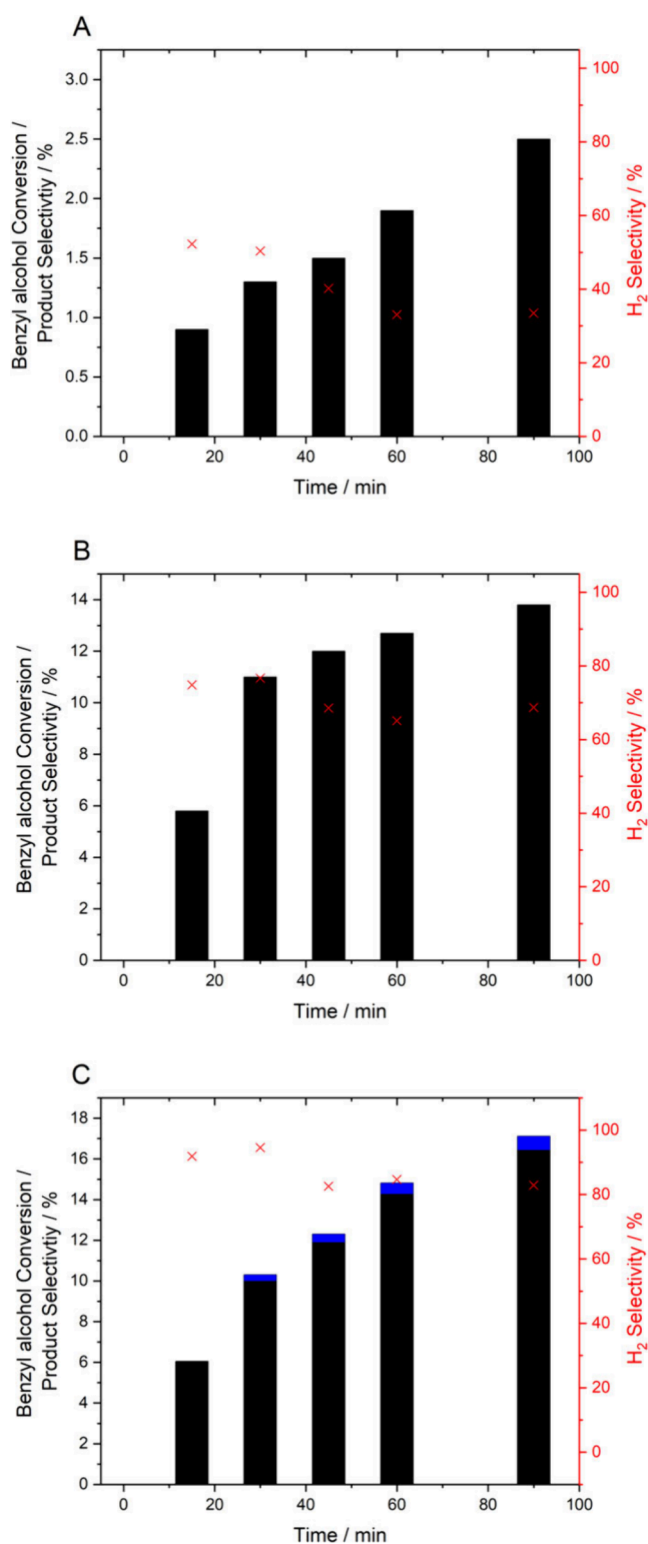
Figure 4. Catalytic performance of (A) 1%Pd/Al$_2$O$_3$, (B) 0.5%Pd-0.5%Au/Al$_2$O$_3$, and (C) 0.5%Pd-0.5%Fe/Al$_2$O$_3$ catalysts toward the selective oxidation of benzyl alcohol via the in situ production of H$_2$O$_2$, as a function of reaction time. Key: benzaldehyde (black bars), benzoic acid (blue bars), H$_2$ selectivity toward benzaldehyde (red crosses). Reaction conditions: catalyst (0.01 g), benzyl alcohol (1.04 g, 9.62 mmol), MeOH (7.1 g), 5% H$_2$/CO$_2$ (420 psi), 25% O$_2$/CO$_2$ (160 psi), 50 °C, 1200 rpm. Note: H$_2$ selectivity was determined based on the mol of H$_2$ utilized in the formation of benzaldehyde.
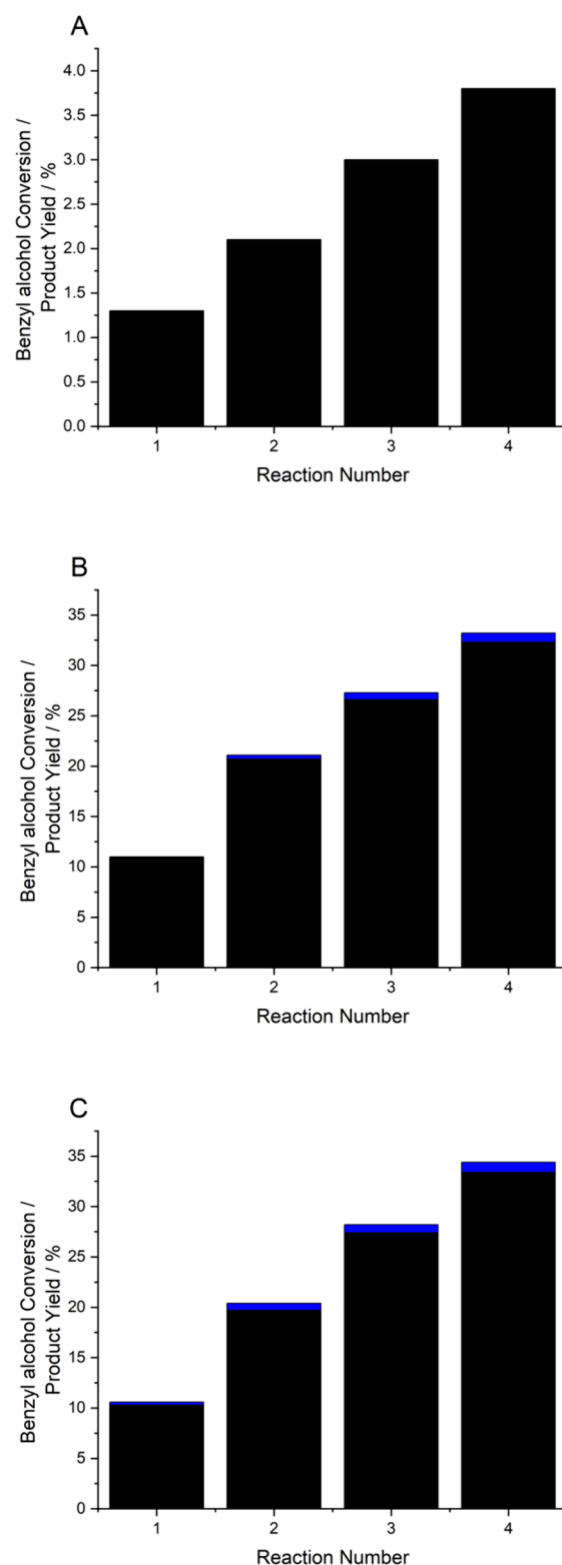
Figure 5. Catalytic performance of (A) 1%Pd/Al$_2$O$_3$, (B) 0.5%Pd-0.5%Au/Al$_2$O$_3$, and (C) 0.5%Pd-0.5%Fe/Al$_2$O$_3$ catalysts toward the selective oxidation of benzyl alcohol via the in situ synthesis of H$_2$O$_2$, over sequential reactions. Key: benzaldehyde (black bars), benzoic acid (blue bars), selectivity based on H$_2$ (red cross). Reaction conditions: catalyst (0.01 g), benzyl alcohol (1.04 g, 9.62 mmol), MeOH (7.1 g), 5% H$_2$/CO$_2$ (420 psi), 25% O$_2$/CO$_2$ (160 psi), 50 °C, 1200 rpm.
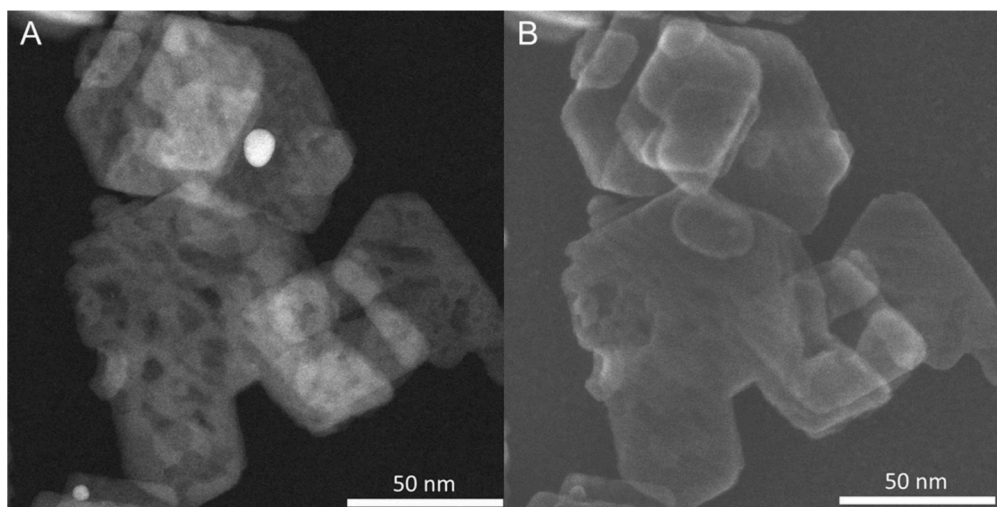
Figure 6. (A) Representative STEM-HAADF and (B) secondary electron micrographs of the as-prepared 1%Pd/Al$_2$O$_3$ catalyst, showing the presence of relatively large nanoparticles.

The formation of PdAu nanoalloys has long been known to improve catalytic selectivity toward H$_2$O$_2$ in comparison to Pd-only analogues, with O−O bond dissociation and the formation of water suppressed over bi-metallic PdAu surfaces.[14] Recently we have also demonstrated that the introduction of Au may promote the release of intermediate species (i.e., O$_2^{\bullet-}$, $^\bullet$OH, and $^\bullet$OOH) generated during H$_2$O$_2$ direct synthesis.[15] The formation of such reactive oxygen species can be directly related to the improved performance of PdAu catalysts over monometallic Pd analogues for many selective oxidative processes, where H-abstraction is a key step in the catalysis.[31] However, unlike PdAu catalysts the formation of oxygen-based radicals over PdFe formulations may be predominantly related to a combination of the H$_2$O$_2$ synthesizing activity of Pd and subsequent Fe-catalyzed Fenton-type pathways. Indeed, the bi-functional nature of PdFe catalysts has been previously utilized for both selective and total oxidative transformations, via oxygen-based radical species.[17,55]

Owing to the well-known ability of methanol (the solvent used in this study) to act as a radical scavenger, and focusing on the PdAu and PdFe formulations, we conducted a series of spin-trapping Electron Paramagnetic Resonance (EPR) spectroscopy measurements, using 5,5-dimethyl-1-pyrroline N-oxide (DMPO) as the radical trapping agent, in order to determine the extent of ROS generation over these two catalysts (Figure 8A). Notably these initial experiments were conducted in the presence of a water-only solvent and the absence of the benzyl alcohol substrate, in order to avoid contributions from alternative radical species (e.g., CH$_3$O$^\bullet$ and PhCH$^\bullet$(OH)). In the case of the 0.5%Pd-0.5%Au/Al$_2$O$_3$ catalyst, the EPR spectrum was dominated by a signal symptomatic of a DMPO−OH radical adduct (g_{iso} = 2.006, a_{iso}(^{14}N) = 1.493 mT, and a_{iso}(^{1}H$_\beta$) = 1.493 mT), which could arise from the trapping of an oxygen centered radicals ($^\bullet$OH and $^\bullet$OOH), indicating the formation of oxygen based radical species (ROS). Notably, it was not possible to distinguish between trapped $^\bullet$OH and $^\bullet$OOH species due to the short half-life of the DMPO−OOH adduct, which rapidly decays to DMPO−OH in the presence of unreacted DMPO. Subsequent quantification of these ROS (in the form of the DMPO−OH adduct) via double integration from spin-trapping EPR data in

conjunction with the calibration curves reported in Figure S12 suggests a relatively low concentration of ROS. By comparison, no signal associated with ROS was detected in the presence of the 0.5%Pd-0.5%Fe/Al$_2$O$_3$ catalyst. Such observations may be surprising, however, subsequent H$_2$O$_2$ synthesis experiments, using a water-only reaction medium, revealed the decreased activity of both catalysts, but particularly the PdFe formulation, toward H$_2$O$_2$ production in the absence of methanol (Table S12). This in part can be attributed to the improved solubility of gaseous reagents in methanol compared to water.

It is well-known that the solvent is not fully innocent within the direct synthesis reaction, with earlier studies highlighting that improved H$_2$O$_2$ synthesis rates may be achieved through the use of protic solvents.[56] Indeed, MeOH-containing solvents offer increased catalytic performance in comparison to the use of a water-only based reaction medium (Table S12).[24] EPR spectra gathered in the presence of the methanol solvent (and absence of benzyl alcohol) revealed a clear signal which may be attributed to a DMPO-OCH$_3$ aminoxyl radical adduct with g_{iso} = 2.006, a_{iso}(^{14}N) = 1.36 mT, and a_{iso}(^{1}H$_\beta$) = 0.8 mT, which is in agreement with previously reported hyperfine coupling values.[57] Notably, no signal associated with ROS were observed, which is perhaps unsurprising given the high concentrations of methanol, compared to DMPO, in the system and the ability of methanol to scavenge ROS.

Quantification of the aminoxyl radical adduct through double integration of the EPR spectra, in conjunction with the calibration curves reported in Figure S13, indicates a stark difference in aminoxyl radical generation over the 0.5%Pd-0.5%Au/Al$_2$O$_3$ and 0.5%Pd-0.5%Fe/Al$_2$O$_3$ formulations (0.03 versus 0.46 μM for the PdAu and PdFe catalysts, respectively). The EPR spectra in Figure 8 are difficult to reconcile in terms of ROS radical scavenging by methanol generated methoxyl radicals that are trapped by DMPO, given that in water, the 0.5%Pd-0.5%Fe/Al$_2$O$_3$ has not shown any evidence of DMPO−OH adducts, and only the 0.5%Pd-0.5%Au/Al$_2$O$_3$ catalyst did reveal this adduct signal. It is likely that the routes to DMPO-OCH$_3$ adduct formation are numerous and complex (proposed reaction pathways that lead to the generation of ROS over the PdAu and PdFe catalysts are shown in Figure 9). While our EPR analysis may indicate that oxygen-based radicals, generated via H$_2$O$_2$ synthesis (or degradation
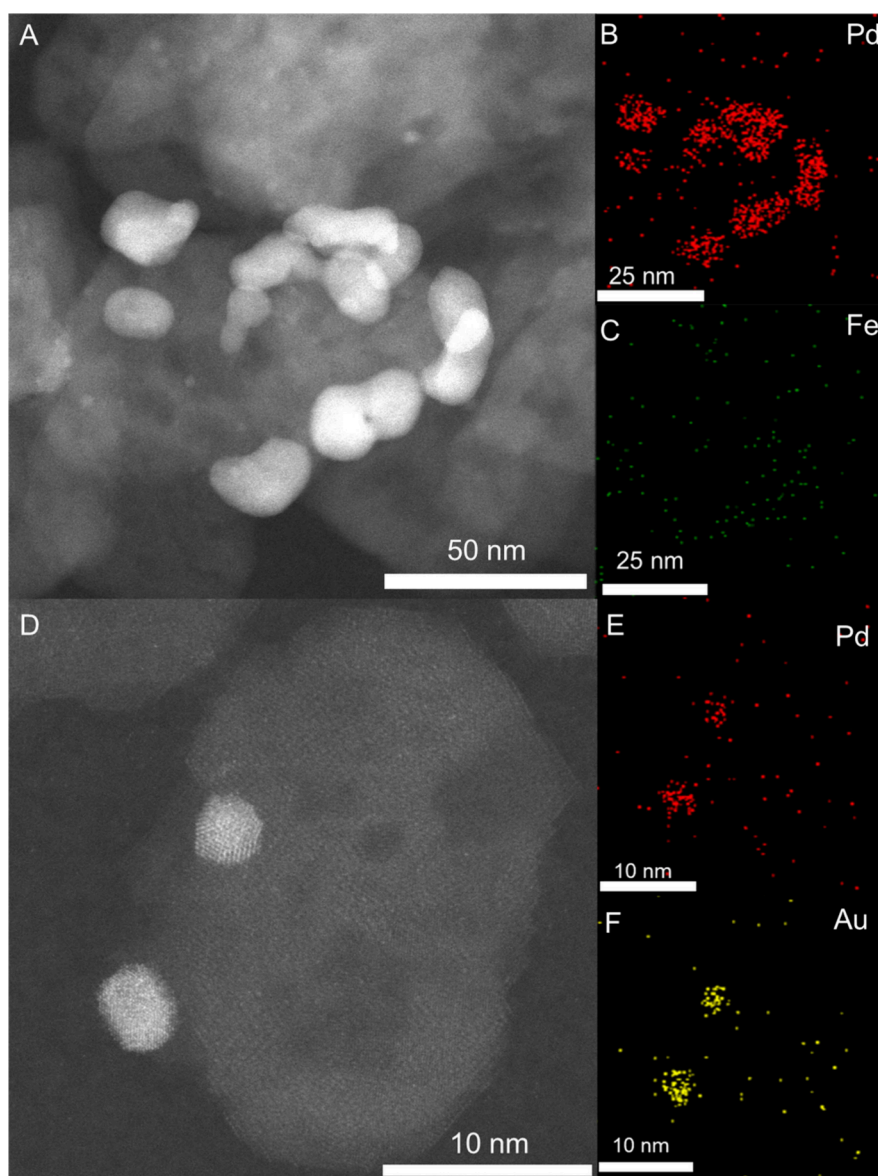
Figure 7. HAADF-STEM and X-EDS imaging of the as-prepared PdFe and PdAu catalysts. (A) Analysis of 0.5%Pd-0.5%Fe/Al$_2$O$_3$ catalyst, highlighting the presence of Pd-dominated larger agglomerates and nanoparticles. (B) Pd and (C) Fe XEDS maps of the area shown in (A). (D) Analysis of the 0.5%Pd-0.5%Au/Al$_2$O$_3$ catalyst, indicating the presence of PdAu nanoalloys. (E) Pd and (F) Au XEDS maps of the area shown in (D) (additional data reported in Figures S8−11).

pathways) are the primary reactive species, it is not clear if the methoxy-based species (whether directly generated and trapped by DMPO) play a dominant role in the catalysis or simply propagate a radical chain reaction. Indeed, given the considerable difference in the concentration of methoxy radicals generated over the two bimetallic formulations but similar rates of benzyl alcohol conversion observed in our in situ experiments, it is possible that such species are purely spectators.

CONCLUSION

The in situ synthesis and utilization of H$_2$O$_2$ (and associated oxygen-based radicals) in the low-temperature valorization of benzyl alcohol offers significantly improved efficacy when compared to purely aerobic routes or when utilizing commercial H$_2$O$_2$. In particular, the incorporation of Fe and Au into a supported Pd/Al$_2$O$_3$ catalyst has been found to dramatically increase catalytic performance. Evaluation of catalyst activity toward H$_2$O$_2$ direct synthesis, benzyl alcohol oxidation in the presence of preformed H$_2$O$_2$ and analysis by EPR spectroscopy indicates that reactive oxygen-based species (ROS), rather than H$_2$O$_2$ are primarily responsible for the observed catalysis. While the origins of all these oxygen-based radicals are not fully understood, it is hypothesized that they are generated primarily as reaction intermediates formed during H$_2$O$_2$ synthesis over PdAu surfaces, while Fenton-type pathways are considered to be the dominant route to their formation over PdFe analogues. Notably, the solvent (methanol) was found to be noninnocent, with methoxy radicals also detected via EPR. However, the extent to which these species are involved in the oxidation of benzyl alcohol is not clear, and one can hypothesize that they contribute to the initial proton-abstraction from the alcohol moiety (PhCH$_2$O*H*) or may act as a propagating agent for subsequent
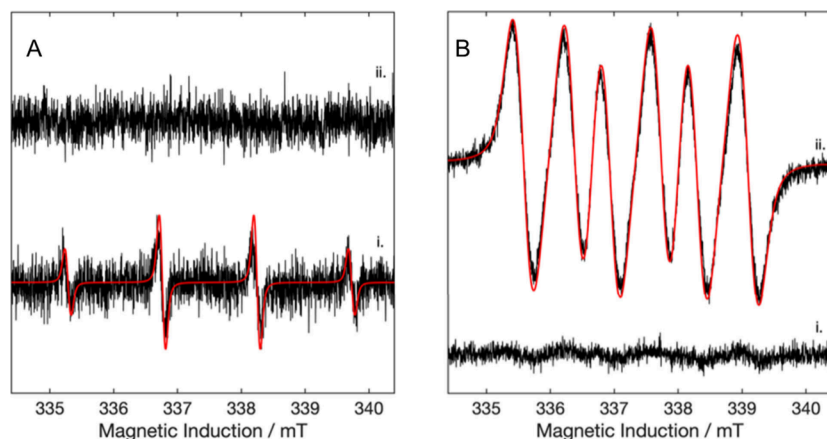
Figure 8. Experimental (black) and simulated (red) CW-EPR spectra of DMPO-radical adducts formed during the in situ oxidation of benzyl alcohol. (A) Reactions conducted in water at 50 °C, in the absence of benzyl alcohol in the presence of DMPO (i) 1%PdAu/Al$_2$O$_3$ and (ii) 1% PdFe/Al$_2$O$_3$. (B) Reactions conducted in methanol at 50 °C, in the absence of benzyl alcohol and in the presence of DMPO (i) 1%PdAu/Al$_2$O$_3$ and (ii) 1% PdFe/Al$_2$O$_3$. Reaction conditions: catalyst (0.01 g), solvent (7.1 g), 5%H$_2$/CO$_2$ (420 psi), 25%O$_2$/CO$_2$ (160 psi), 0.5 h, 50 °C, 1200 rpm.
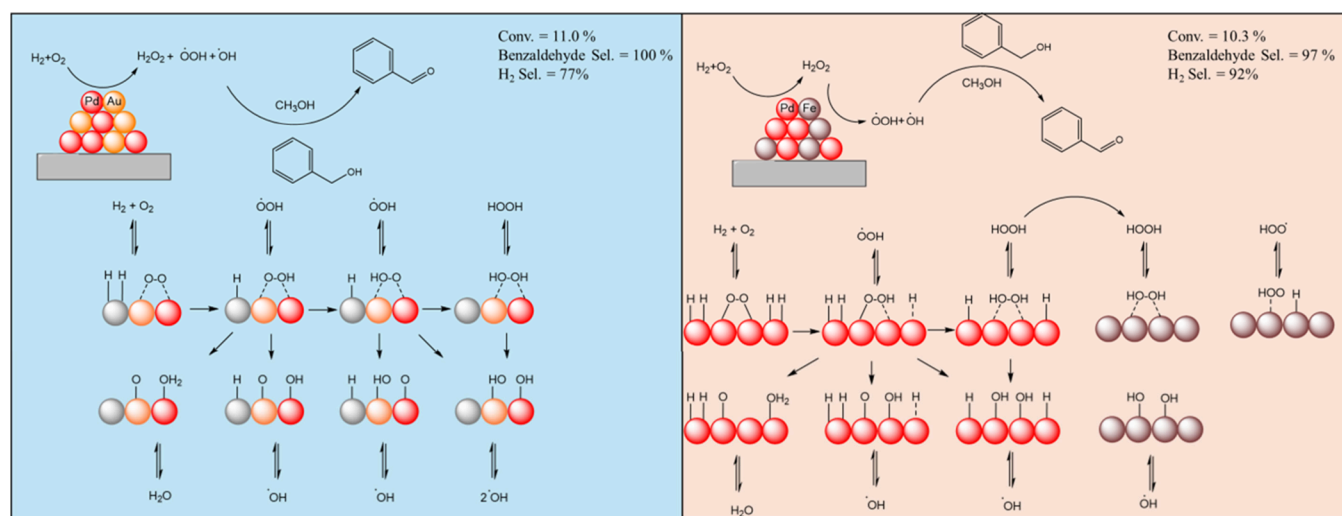
Figure 9. Proposed reaction pathways involved in the formation of reactive oxygen species during the in situ oxidation of benzyl alcohol.

ROS formation. Nevertheless, the similar performance of key bimetallic catalysts toward in situ benzyl alcohol oxidation, despite a near 20-fold variation in the concentration of O-centered methoxy radicals, may indicate that such species play no role in the catalysis.

Notably, both the PdAu and PdFe bimetallic catalyst formulations significantly outperform those previously reported in the literature, however, the incorporation of Fe, in particular, was found to offer enhanced utilization of H$_2$, outperforming the PdAu or indeed the Pd-only analogue. Such observations are particularly promising given the need to achieve high H$_2$ efficiency if an in situ approach is to rival current industrial technologies, although it is clear further improvements in catalytic reactivity must also be realized.

ASSOCIATED CONTENT

Supporting Information

The Supporting Information is available free of charge at https://pubs.acs.org/doi/10.1021/acscatal.4c04698.

Data relating to catalytic activity toward the direct synthesis and subsequent degradation of H$_2$O$_2$ and the

in situ oxidation of benzyl alcohol to the corresponding aldehyde, with accompanying characterization of catalytic materials via XRD, BET, XPS, CO-DRIFTS, HAADF-STEM, and X-EDS (PDF)

AUTHOR INFORMATION

Corresponding Authors

Richard J. Lewis − *Max Planck-Cardiff Centre on the Fundamentals of Heterogeneous Catalysis FUNCAT, Cardiff Catalysis Institute, School of Chemistry, Cardiff University, Translational Research Hub, Cardiff CF24 4HQ, United Kingdom;* orcid.org/0000-0001-9990-7064; Email: LewisR27@Cardiff.ac.uk

Xi Liu − *In-situ Centre for Physical Sciences, School of Chemistry and Chemical, Frontiers Science Centre for Transformative Molecules, Shanghai 200240, P. R. China;* orcid.org/0000-0002-8654-0774; Email: LiuXi@edu.cn

Graham J. Hutchings − *Max Planck-Cardiff Centre on the Fundamentals of Heterogeneous Catalysis FUNCAT, Cardiff Catalysis Institute, School of Chemistry, Cardiff University, Translational Research Hub, Cardiff CF24 4HQ, United*

Kingdom; orcid.org/0000-0001-8885-1560;
Email: Hutch@Cardiff.ac.uk

Authors

Gregory Sharp − *Max Planck-Cardiff Centre on the Fundamentals of Heterogeneous Catalysis FUNCAT, Cardiff Catalysis Institute, School of Chemistry, Cardiff University, Translational Research Hub, Cardiff CF24 4HQ, United Kingdom*

Junhong Liu − *In-situ Centre for Physical Sciences, School of Chemistry and Chemical, Frontiers Science Centre for Transformative Molecules, Shanghai 200240, P. R. China*

Guiseppina Magri − *School of Chemistry, Cardiff University, Cardiff CF10 3AT, United Kingdom*

David J. Morgan − *Max Planck-Cardiff Centre on the Fundamentals of Heterogeneous Catalysis FUNCAT, Cardiff Catalysis Institute, School of Chemistry, Cardiff University, Translational Research Hub, Cardiff CF24 4HQ, United Kingdom; HarwellXPS, Research Complex at Harwell (RCaH), Didcot OX11 0FA, United Kingdom;* orcid.org/0000-0002-6571-5731

Thomas E. Davies − *Max Planck-Cardiff Centre on the Fundamentals of Heterogeneous Catalysis FUNCAT, Cardiff Catalysis Institute, School of Chemistry, Cardiff University, Translational Research Hub, Cardiff CF24 4HQ, United Kingdom*

Ángeles López-Martín − *Max Planck-Cardiff Centre on the Fundamentals of Heterogeneous Catalysis FUNCAT, Cardiff Catalysis Institute, School of Chemistry, Cardiff University, Translational Research Hub, Cardiff CF24 4HQ, United Kingdom*

Rong-Jian Li − *Max Planck-Cardiff Centre on the Fundamentals of Heterogeneous Catalysis FUNCAT, Cardiff Catalysis Institute, School of Chemistry, Cardiff University, Translational Research Hub, Cardiff CF24 4HQ, United Kingdom;* orcid.org/0000-0002-3514-4931

Callum R. Morris − *Net Zero Innovation Institute, Cardiff Catalysis Institute, School of Chemistry, Cardiff University, Translational Research Hub, Cardiff CF24 4HQ, United Kingdom*

Damien M. Murphy − *School of Chemistry, Cardiff University, Cardiff CF10 3AT, United Kingdom;* orcid.org/0000-0002-5941-4879

Andrea Folli − *Net Zero Innovation Institute, Cardiff Catalysis Institute, School of Chemistry, Cardiff University, Translational Research Hub, Cardiff CF24 4HQ, United Kingdom;* orcid.org/0000-0001-8913-6606

A. Iulian Dugulan − *Laboratory of Fundamentals Aspects of Materials and Energy, Department of Radiation Science & Technology, Delft University of Technology, 2628 CD Delft, The Netherlands*

Liwei Chen − *In-situ Centre for Physical Sciences, School of Chemistry and Chemical, Frontiers Science Centre for Transformative Molecules, Shanghai 200240, P. R. China*

Complete contact information is available at:
https://pubs.acs.org/10.1021/acscatal.4c04698

Author Contributions

△G.S. and R.J.L. contributed equally to this work.

Author Contributions

G.S., R.J.L., and R.L. conducted catalyst synthesis, testing, and corresponding data analysis. G.S., R.J.L., J.L., G.M., D.J.M., T.E.D., A.L., A.I.D., and X.L. conducted catalyst character-ization and corresponding data processing. D.M.M., A.F., C.R.M., A.I.D., and X.L. provided technical advice. R.J.L. and G.J.H. contributed to the design of the study and result interpretation. R.J.L. wrote the manuscript and Supporting Information, with all authors commenting on and amending both documents. All authors discussed and contributed to this work.

Notes

The authors declare no competing financial interest.

REFERENCES

(1) Puértolas, B.; Hill, A. K.; García, T.; Solsona, B.; Torrente-Murciano, L. In-situ synthesis of hydrogen peroxide in tandem with selective oxidation reactions: A mini-review. *Catal. Today* **2015**, *248*, 115−127.

(2) Lewis, R. J.; Ueura, K.; Liu, X.; Fukuta, Y.; Davies, T. E.; Morgan, D. J.; Chen, L.; Qi, J.; Singleton, J.; Edwards, J. K.; Freakley, S. J.; Kiely, C. J.; Yamamoto, Y.; Hutchings, G. J. Highly efficient catalytic production of oximes from ketones using in situ-generated H$_2$O$_2$. *Science* **2022**, *376* (6593), 615−620.

(3) Della Pina, C.; Falletta, E.; Rossi, M. Highly selective oxidation of benzyl alcohol to benzaldehyde catalyzed by bimetallic gold−copper catalyst. *J. Catal.* **2008**, *260* (2), 384−386.

(4) Nagy, G.; Gál, T.; Srankó, D. F.; Sáfrán, G.; Maróti, B.; Sajó, I. E.; Schmidt, F. P.; Beck, A. Selective aerobic oxidation of benzyl alcohol on alumina supported Au-Ru and Au-Ir catalysts. *Mol. Catal.* **2020**, *492*, 110917.

(5) Xiao, Y.; Liang, L.; Liu, Z.; Yin, X.; Yang, X.; Ding, Y.; Du, Z. Facile fabrication of size-controlled Pd nanoclusters supported on Al$_2$O$_3$ as excellent catalyst for solvent-free aerobic oxidation of benzyl alcohol. *Appl. Surf. Sci.* **2022**, *585*, 152668.

(6) Sun, J.; Han, Y.; Fu, H.; Qu, X.; Xu, Z.; Zheng, S. Au@Pd/TiO$_2$ with atomically dispersed Pd as highly active catalyst for solvent-free aerobic oxidation of benzyl alcohol *Chem. Eng. J.* **2017**, *313*, 1−9.

(7) Zhang, J.; Xiao, S.; Chen, R.; Chen, F. Promotional effect of short-chain saturated alcohols on Fe$_3$O$_4$-catalyzed decomposition of H$_2$O$_2$ and its application in selective oxidation of benzyl alcohol. *J. Chem. Technol. Biotechnol.* **2019**, *94* (5), 1613−1621.

(8) Zhao, Y.; Yu, C.; Wu, S.; Zhang, W.; Xue, W.; Zeng, Z. Synthesis of Benzaldehyde and Benzoic Acid by Selective Oxidation of Benzyl Alcohol with Iron(III) Tosylate and Hydrogen Peroxide: A Solvent-Controlled Reaction. *Catal. Lett.* **2018**, *148* (10), 3082−3092.

(9) Lewis, R. J.; Ueura, K.; Fukuta, Y.; Davies, T. E.; Morgan, D. J.; Paris, C. B.; Singleton, J.; Edwards, J. K.; Freakley, S. J.; Yamamoto, Y.; Hutchings, G. J. Cyclohexanone ammoximation via in situ H$_2$O$_2$ production using TS-1 supported catalysts. *Green Chem.* **2022**, *24*, 9496−9507.

(10) Jin, Z.; Wang, L.; Zuidema, E.; Mondal, K.; Zhang, M.; Zhang, J.; Wang, C.; Meng, X.; Yang, H.; Mesters, C.; Xiao, F. Hydrophobic zeolite modification for in situ peroxide formation in methane oxidation to methanol. *Science* **2020**, *367* (6474), 193−197.

(11) Ricciardulli, T.; Gorthy, S.; Adams, J. S.; Thompson, C.; Karim, A. M.; Neurock, M.; Flaherty, D. W. Effect of Pd coordination and isolation on the catalytic reduction of O2 to H_2O_2 over PdAu bimetallic nanoparticles. *J. Am. Chem. Soc.* **2021**, *143* (14), 5445−5464.

(12) Wilson, N. M.; Priyadarshini, P.; Kunz, S.; Flaherty, D. W. Direct synthesis of H_2O_2 on Pd and Au_xPd_1 clusters: Understanding the effects of alloying Pd with Au. *J. Catal.* **2018**, *357*, 163−175.

(13) Edwards, J. K.; Solsona, B.; N, E. N.; Carley, A. F.; Herzing, A. A.; Kiely, C. J.; Hutchings, G. J. Switching off hydrogen peroxide hydrogenation in the direct synthesis process. *Science* **2009**, *323*, 1037−1041.

(14) Li, J.; Ishihara, T.; Yoshizawa, K. Theoretical Revisit of the Direct Synthesis of H_2O_2 on Pd and Au@Pd Surfaces: A Comprehensive Mechanistic Study. *J. Phys. Chem. C* **2011**, *115*, 25359−25367.

(15) Richards, T.; Harrhy, J. H.; Lewis, R. J.; Howe, A. G. R.; Suldecki, G. M.; Folli, A.; Morgan, D. J.; Davies, T. E.; Loveridge, E. J.; Crole, D. A.; Edwards, J. K.; Gaskin, P.; Kiely, C. J.; He, Q.; Murphy, D. M.; Maillard, J.-Y.; Freakley, S. J.; Hutchings, G. J. A residue-free approach to water disinfection using catalytic in situ generation of reactive oxygen species. *Nat. Catal.* **2021**, *4* (7), 575−585.

(16) Yang, G. S.; Kang, J.; Park, E. D. Aqueous-Phase Partial Oxidation of Methane over Pd−Fe/ZSM-5 with O2 in the Presence of H_2. *ChemCatChem.* **2023**, *15* (7), No. e202201630.

(17) Santos, A.; Lewis, R. J.; Morgan, D. J.; Davies, T. E.; Hampton, E.; Gaskin, P.; Hutchings, G. J. The oxidative degradation of phenol via in situ H_2O_2 synthesis using Pd supported Fe-modified ZSM-5 catalysts. *Catal. Sci. Technol.* **2022**, *12* (9), 2943−2953.

(18) Underhill, R.; Douthwaite, M.; Lewis, R. J.; Miedziak, P. J.; Armstrong, R. D.; Morgan, D. J.; Freakley, S. J.; Davies, T.; Folli, A.; Murphy, D. M.; He, Q.; Akdim, O.; Edwards, J. K.; Hutchings, G. J. Ambient base-free glycerol oxidation over bimetallic PdFe/SiO_2 by in situ generated active oxygen species. *Res. Chem. Intermed.* **2021**, *47* (1), 303−324.

(19) Crombie, C. M.; Lewis, R. J.; Taylor, R. L.; Morgan, D. J.; Davies, T. E.; Folli, A.; Murphy, D. M.; Edwards, J. K.; Qi, J.; Jiang, H.; Kiely, C. J.; Liu, X.; Skjøth-Rasmussen, M. S.; Hutchings, G. J. Enhanced Selective Oxidation of Benzyl Alcohol via In Situ H_2O_2 Production over Supported Pd-Based Catalysts. *ACS Catal.* **2021**, *11* (5), 2701−2714.

(20) Lewis, R. J.; Ueura, K.; Liu, X.; Fukuta, Y.; Qin, T.; Davies, T. E.; Morgan, D. J.; Stenner, A.; Singleton, J.; Edwards, J. K.; Freakley, S. J.; Kiely, C. J.; Chen, L.; Yamamoto, Y.; Hutchings, G. J. Selective Ammoximation of Ketones via In Situ H_2O_2 Synthesis. *ACS Catal.* **2023**, *13* (3), 1934−1945.

(21) Brehm, J.; Lewis, R. J.; Morgan, D. J.; Davies, T. E.; Hutchings, G. J. The direct synthesis of hydrogen peroxide over AuPd nanoparticles: an investigation into metal loading. *Catal. Lett.* **2022**, *152* (1), 254−262.

(22) Sankar, M.; He, Q.; Morad, M.; Pritchard, J.; Freakley, S. J.; Edwards, J. K.; Taylor, S. H.; Morgan, D. J.; Carley, A. F.; Knight, D. W.; Kiely, C. J.; Hutchings, G. J. Synthesis of stable ligand-free gold−palladium nanoparticles using a simple excess anion method. *ACS Nano* **2012**, *6*, 6600.

(23) Hu, X.; Xie, Q.; Zhang, J.; Yu, Q.; Liu, H.; Sun, Y. Experimental study of the lower flammability limits of $H_2/O_2/CO_2$ mixture. *Int. J. Hydrogen Energy* **2020**, *45* (51), 27837−27845.

(24) Santos, A.; Lewis, R. J.; Malta, G.; Howe, A. G. R.; Morgan, D. J.; Hampton, E.; Gaskin, P.; Hutchings, G. J. Direct synthesis of hydrogen peroxide over Au−Pd supported nanoparticles under ambient conditions. *Ind. Eng. Chem. Res.* **2019**, *58* (28), 12623−12631.

(25) Edwards, J. K.; Thomas, A.; Carley, A. F.; Herzing, A. A.; Kiely, C. J.; Hutchings, G. J. Au−Pd supported nanocrystals as catalysts for the direct synthesis of hydrogen peroxide from H_2 and O_2. *Green Chem.* **2008**, *10* (4), 388−394.

(26) Stoll, S.; Schweiger, A. EasySpin, a comprehensive software package for spectral simulation and analysis in EPR. *J. Magn. Reson.* **2006**, *178* (1), 42−55.

(27) Klencsár, Z. Mössbauer spectrum analysis by evolution algorithm. *Nucl. Instrum. Methods Phys. Res.* **1997**, *129* (4), 527−533.

(28) Ntainjua N, E.; Edwards, J. K.; Carley, A. F.; Lopez-Sanchez, J. A.; Moulijn, J. A.; Herzing, A. A.; Kiely, C. J.; Hutchings, G. J. The role of the support in achieving high selectivity in the direct formation of hydrogen peroxide. *Green Chem.* **2008**, *10*, 1162−1169.

(29) Richards, T.; Lewis, R. J.; Morgan, D. J.; Hutchings, G. J. The Direct Synthesis of Hydrogen Peroxide Over Supported Pd-Based Catalysts: An Investigation into the Role of the Support and Secondary Metal Modifiers. *Catal. Lett.* **2023**, *153*, 32−40.

(30) Biasi, P.; Menegazzo, F.; Pinna, F.; Eränen, K.; Salmi, T. O.; Canu, P. Continuous H_2O_2 direct synthesis over PdAu catalysts. *Chem. Eng. J.* **2011**, *176−177*, 172−177.

(31) Ni, F.; Richards, T.; Smith, L. R.; Morgan, D. J.; Davies, T. E.; Lewis, R. J.; Hutchings, G. J. Selective Oxidation of Methane to Methanol via In Situ H_2O_2 Synthesis. *ACS Org. Inorg. Au* **2023**, *3* (4), 177−183.

(32) Wu, P.; Cao, Y.; Zhao, L.; Wang, Y.; He, Z.; Xing, W.; Bai, P.; Mintova, S.; Yan, Z. Formation of PdO on Au−Pd bimetallic catalysts and the effect on benzyl alcohol oxidation. *J. Catal.* **2019**, *375*, 32−43.

(33) Guan, W.; Zhang, Y.; Yan, C.; Chen, Y.; Wei, Y.; Cao, Y.; Wang, F.; Huo, P. Base-Free Aerobic Oxidation of Furfuralcohols and Furfurals to Furancarboxylic Acids over Nitrogen-Doped Carbon-Supported AuPd Bowl-Like Catalyst. *ChemSusChem* **2022**, *15* (16), No. e202201041.

(34) Nishimura, S.; Yakita, Y.; Katayama, M.; Higashimine, K.; Ebitani, K. The role of negatively charged Au states in aerobic oxidation of alcohols over hydrotalcite supported AuPd nanoclusters. *Catal. Sci. Technol.* **2013**, *3* (2), 351−359.

(35) Wan, X.; Zhou, C.; Chen, J.; Deng, W.; Zhang, Q.; Yang, Y.; Wang, Y. Base-Free Aerobic Oxidation of 5-Hydroxymethyl-furfural to 2,5-Furandicarboxylic Acid in Water Catalyzed by Functionalized Carbon Nanotube-Supported Au−Pd Alloy Nanoparticles. *ACS Catal.* **2014**, *4* (7), 2175−2185.

(36) Guo, S.; Zhang, S.; Fang, Q.; Abroshan, H.; Kim, H. J.; Haruta, M.; Li, G. Gold−Palladium Nanoalloys Supported by Graphene Oxide and Lamellar TiO_2 for Direct Synthesis of Hydrogen Peroxide. *ACS Appl. Mater. Interfaces* **2018**, *10* (47), 40599−40607.

(37) Nowicka, E.; Althahban, S.; Leah, T. D.; Shaw, G.; Morgan, D.; Kiely, C. J.; Roldan, A.; Hutchings, G. J. Benzyl alcohol oxidation with Pd-Zn/TiO_2: computational and experimental studies. *Sci. Technol. Adv. Mater.* **2019**, *20* (1), 367−378.

(38) Marakatti, V. S.; Sarma, S. C.; Joseph, B.; Banerjee, D.; Peter, S. C. Synthetically tuned atomic ordering in PdCu nanoparticles with enhanced catalytic activity toward solvent-free benzylamine oxidation. *ACS Appl. Mater. Interfaces* **2017**, *9* (4), 3602−3615.

(39) Freakley, S. J.; He, Q.; Harrhy, J. H.; Lu, L.; Crole, D. A.; Morgan, D. J.; Ntainjua, E. N.; Edwards, J. K.; Carley, A. F.; Borisevich, A. Y.; Kiely, C. J.; Hutchings, G. J. Palladium-tin catalysts for the direct synthesis of H_2O_2 with high selectivity. *Science* **2016**, *351*, 965−968.

(40) Cao, K.; Yang, H.; Bai, S.; Xu, Y.; Yang, C.; Wu, Y.; Xie, M.; Cheng, T.; Shao, Q.; Huang, X. Efficient Direct H_2O_2 Synthesis Enabled by PdPb Nanorings via Inhibiting the O−O Bond Cleavage in O_2 and H_2O_2. *ACS Catal.* **2021**, *11* (3), 1106−1118.

(41) Crole, D. A.; Underhill, R.; Edwards, J. K.; Shaw, G.; Freakley, S. J.; Hutchings, G. J.; Lewis, R. J. The direct synthesis of hydrogen peroxide from H_2 and O_2 using Pd−Ni/TiO_2 catalysts. *Philos. Trans. R. Soc., A* **2020**, *378* (2176), 20200062.

(42) Wang, S.; Doronkin, D. E.; Hähsler, M.; Huang, X.; Wang, D.; Grunwaldt, J.-D.; Behrens, S. Palladium-Based Bimetallic Nanocrystal

Catalysts for the Direct Synthesis of Hydrogen Peroxide. *ChemSusChem* **2020**, *13* (12), 3243−3251.

(43) Kovačič, D.; Lewis, R. J.; Crombie, C. M.; Morgan, D. J.; Davies, T. E.; López-Martín, Á.; Qin, T.; Allen, C. S.; Edwards, J. K.; Chen, L.; Skjøth-Rasmussen, M. S.; Liu, X.; Hutchings, G. J. A comparative study of palladium-gold and palladium-tin catalysts in the direct synthesis of H$_2$O$_2$. *Green Chem.* **2023**, *25* (24), 10436−10446.

(44) Lewis, R. J.; Hutchings, G. J. Recent Advances in the Direct Synthesis of H2O2. *ChemCatChem.* **2019**, *11*, 298−308.

(45) Sankar, M.; Dimitratos, N.; Miedziak, P. J.; Wells, P. P.; Kiely, C. J.; Hutchings, G. J. Designing bimetallic catalysts for a green and sustainable future. *Chem. Soc. Rev.* **2012**, *41* (24), 8099−8139.

(46) Enache, D. I.; Barker, D.; Edwards, J. K.; Taylor, S. H.; Knight, D. W.; Carley, A. F.; Hutchings, G. J. Solvent-free oxidation of benzyl alcohol using titania-supported gold−palladium catalysts: effect of Au−Pd ratio on catalytic performance. *Catal. Today* **2007**, *122* (3), 407−411.

(47) Enache, D. I.; Edwards, J. K.; Landon, P.; Solsona-Espriu, B.; Carley, A. F.; Herzing, A. A.; Watanabe, M.; Kiely, C. J.; Knight, D. W.; Hutchings, G. J. Solvent-free oxidation of primary alcohols to aldehydes using Au-Pd/TiO$_2$ catalysts. *Science* **2006**, *311*, 362−365.

(48) Tang, C.; Zhang, N.; Shao, Q.; Huang, X.; Xiao, X. Rational design of ordered Pd−Pb nanocubes as highly active, selective and durable catalysts for solvent-free benzyl alcohol oxidation. *Nanoscale* **2019**, *11* (12), 5145−5150.

(49) Santonastaso, M.; Freakley, S. J.; Miedziak, P. J.; Brett, G. L.; Edwards, J. K.; Hutchings, G. J. Oxidation of benzyl alcohol using in situ generated hydrogen peroxide. *Org. Process Res. Dev.* **2014**, *18* (11), 1455−1460.

(50) Scoville, J. R.; Novicova, I. A. (assigned to COTTRELL MERGING CORP Metrex Research LLC.) Hydrogen peroxide disinfecting and sterilizing compositions, US5900256A, filing date: 17/02/1996.

(51) Gong, X.; Lewis, R. J.; Zhou, S.; Morgan, D. J.; Davies, T. E.; Liu, X.; Kiely, C. J.; Zong, B.; Hutchings, G. J. Enhanced catalyst selectivity in the direct synthesis of H$_2$O$_2$ through Pt incorporation into TiO$_2$ supported AuPd catalysts. *Catal. Sci. Technol.* **2020**, *10*, 4635−4644.

(52) Sankar, M.; Nowicka, E.; Carter, E.; Murphy, D. M.; Knight, D. W.; Bethell, D.; Hutchings, G. J. The benzaldehyde oxidation paradox explained by the interception of peroxy radical by benzyl alcohol. *Nat. Commun.* **2014**, *5* (1), 3332.

(53) Partenheimer, W. The high yield synthesis of benzaldehydes from benzylic alcohols using homogeneously catalyzed aerobic oxidation in acetic acid. *Adv. Synth. Catal.* **2006**, *348* (4−5), 559−568.

(54) Wang, G.; Du, W.; Duan, X.; Cao, Y.; Zhang, Z.; Xu, J.; Chen, W.; Qian, G.; Yuan, W.; Zhou, X.; Chen, D. Mechanism-guided elaboration of ternary Au−Ti−Si sites to boost propylene oxide formation. *Chem. Catal.* **2021**, *1* (4), 885−895.

(55) Santos, A.; Lewis, R. J.; Morgan, D. J.; Davies, T. E.; Hampton, E.; Gaskin, P.; Hutchings, G. J. The degradation of phenol via in situ H$_2$O$_2$ production over supported Pd-based catalysts. *Catal. Sci. Technol.* **2021**, *11* (24), 7866−7874.

(56) Wilson, N. M.; Flaherty, D. W. Mechanism for the direct synthesis of H$_2$O$_2$ on Pd clusters: heterolytic reaction pathways at the liquid−solid interface. *J. Am. Chem. Soc.* **2016**, *138*, 574−586.

(57) Buettner, G. R. Spin trapping: ESR parameters of spin adducts. *Free Radical Biol. Med.* **1987**, *3* (4), 259−303.